

## ADVANCED MRI PROTOCOL IN EVALUATION AND ASSESSMENT OF BRAIN TUMOR

**Dr AMOL GAUTAM**

PROFESSOR , DEPARTMENT OF RADIODIAGNOSIS  
SYMBIOSIS MEDICAL COLLEGE FOR WOMEN, PUNE

[gautamamol75@gmail.com](mailto:gautamamol75@gmail.com)

**Dr AMOL BHOITE**

ASST. PROFESSOR, DEPARTMENT OF RADIODIAGNOSIS

**DR SUNIL YADAV**

ASSISTANT PROFESSOR  
DEPARTMENT OF NUROSCIENCES  
KRISHNA INSTITUTE OF  
MEDICAL SCIENCES KARAD-415110,  
MAHARASHTRA STATE.

2023

[drsunilyadav76@gmail.com](mailto:drsunilyadav76@gmail.com)

### ABSTRACT:

**Background:** Intracranial tumors are a significant health issue. The annual incidence of primary and secondary central nervous system neoplasms ranges from 10 to 17 per 100,000 persons. Imaging plays an important role in the management and prognostication of intracranial tumors. Magnetic resonance (MR) imaging has emerged as the imaging modality most frequently used to evaluate intracranial tumors, and it continues to have an ever-expanding, multifaceted role.

**Purpose:** To evaluate the Advance brain tumor imaging (MRI) Protocol in Grading brain tumors both intra-axial and extra-axial.

**Methodology:** This prospective study was performed. The population enrolled in the study for final statistical analysis included 40 patients (23 males and 17 females) with ages ranging from 3 to 79 years.

**Results:** In the study, 37 (92.5%) patients showed supratentorial tumor location, and 3 (7.5%) patients showed infratentorial tumor location. On T1-W, 31 (77.5%) patients show a

heterogeneously hypointense signal, 6 (15%) patients show an isointense signal, and 3 (7.5%) patients show a hypointense signal. On T2W, 37 (92.5%) patients show a heterogeneously hyperintense signal, and 3 (7.5%) patients show a hyperintense signal. On FLAIR, 37 (97.5%) patients show a heterogeneously hyperintense signal, and 1 (2.5% of patients) show a hyperintense signal. In the study, 28 (70%) patients showed no diffusion restriction, and 12 (30%) patients showed patchy diffusion restriction. On SWI 9, 22.5 percent of patients have "blooming," and 31 (77.5 percent) have "no blooming," indicating hemorrhage, which is seen in high-grade gliomas. In the post-contrast enhancement study, 17 (42.5%) patients showed patchy enhancement, 8 (20%) patients showed minimal enhancement, 5 (12.5%) patients showed heterogenous enhancement, and 10 (25%) patients showed no enhancement. In the study, there is no significant difference in the mean of age over the grade of a tumor by applying a two-sample t-test, in which the mean age for high-grade gliomas is  $49.8 \pm 19.8$  and for low-grade gliomas is  $38.83 \pm 15.81$ , and we found no significant difference ( $P = 0.05928$ ) in the distribution of grades of tumor in our study.

**Conclusion:** We found that advanced MRI can differentiate brain tumor grades. Perfusion studies, spectroscopy, and diffuse tensor imaging have a substantial association with the degree of malignancy, predicting different grades of tumor compared to standard MRI imaging alone, aiding in management and follow-up. Using sophisticated MRI imaging sequences in brain tumor imaging provides information on malignancy. Non-invasive, easily accessible procedures aid in patient prognosis and minimize unnecessary stereotactic biopsies for low-grade gliomas requiring follow-up. Using sophisticated MRI imaging sequences to differentiate brain tumor grades is critical for patient care.

**Keywords:** a brain tumor, MRI imaging, Perfusion imaging, CBF, DTI

## INTRODUCTION

Intracranial tumors are a significant health issue. The annual incidence of primary and secondary central nervous system neoplasms ranges from 10 to 17 per 100,000 persons.

Imaging plays an important role in the management and prognostication of intracranial tumors. Magnetic resonance (MR) imaging has emerged as the imaging modality most frequently used to evaluate intracranial tumors, and it continues to have an ever-expanding, multifaceted role.

In general, the role of MR imaging in the evaluation of brain tumors is tumor diagnosis and classification, treatment planning, and post-treatment follow-up.

On conventional MR imaging, grade I tumors show no edema or enhancement, grade II tumors show minimal edema and enhancement, grade III tumors show significant edema and heterogenous enhancement, and grade IV tumors show significant edema, heterogenous enhancement, hemorrhage, and necrosis.

Apart from conventional MR imaging techniques, a variety of advanced techniques have a role in clinical practice or are the subject of research. These advanced MRI imaging

techniques provide more than the anatomic information provided by conventional MR imaging sequences, as they can generate physiologic data and information on chemical composition. Perfusion imaging, diffusion-weighted imaging (including diffusion tensor imaging), MR spectroscopy, and largely experimental molecular imaging are among the advanced MRI imaging techniques. Currently, perfusion imaging<sup>(1-4)</sup>, spectroscopy<sup>(1-5)</sup>, and diffuse tensor imaging<sup>(6-11)</sup> are used in the classification of tumors.

The main diagnostic challenge is to distinguish different grades of intra- and extra-axial brain tumors reliably, noninvasively, and quickly to avoid unnecessary biopsies and follow-up imaging studies.

The inclusion of diagnostic information from advanced MR imaging techniques can improve the classification accuracy of conventional anatomic imaging. This thesis focuses on the role of the most commonly used advanced MR imaging techniques-like perfusion imaging, diffuse tensor imaging, and MR spectroscopy-for the diagnosis and differentiation of different grades of brain tumors.

**Aim:**

- ❖ To evaluate the Advance brain tumor imaging (MRI) Protocol in Grading brain tumors both intra-axial and extra-axial.

**Objectives:**

- ❖ To study the T1, T2, FLAIR, DWI, ADC, SWI and T1FS post-contrast sequences
- ❖ To study advanced MRI sequences perfusion, DTI, and spectroscopy.
- ❖ To evaluate the role of these sequences for grading in these intra-axial and extra-axial brain tumors.

**Methodology**

**StudyDesign:**

The study was designed as a two-year prospective observational study.

**StudyPeriodandduration:**

The study was conducted over a period of two years from March 2021 to July 2021.

**Place:**

The study was conducted in the department of Radiodiagnosis, Krishna Institute of Medical Sciences and Hospital, Karad.

**Sourceofdata:**

The patients are referred to our department from our institute and outside the institute.

**Sélection of participants :**

➤ **Inclusion criteria:**

- Diagnosed brain tumors either on CT or outside imaging which includes both intra-axial and extra-axial tumors.
- Newly diagnosed brain tumors in our department.

➤ **Exclusion criteria:**

- If all sequences could not be done due to the non-cooperation of the patient.

Post-operative brain tumor patients and brain metastasis

**Equipment and Technique**

After appropriate preparation and normal creatinine levels, the patients were subjected to conventional and advanced MRI imaging techniques using a 1.5 Tesla machine (SeimensMagnetomAvanto). Conventional T1, T2, FLAIR, DWI & ADC, and SWI sequences are used. The advanced MRI imaging techniques perfusion study, spectroscopy, and diffuse tensor imaging are used.

**Data analysis**

Data are analyzed using statistical software **R version 4.1.1** and **Microsoft Excel**. Continuous variables were represented by mean± sd/median (range) and categorical variables were represented by frequency and percentage. To check the association between categorical variables Chi-square test is used. To check the normality of variables Shapiro-Wilk's test is used. To compare the mean between groups two-sample t-test is used. A P-value less than or equal to 0.05 indicates statistical significance.

**SUMMARY:**

This is a prospective observational study of 40 patients. The study group consists of 23 males and 17 females with a mean age of 43.23 ±18.11. The incidence was higher in males (57.5%) compared to females (42.5%).The below table gives a summary of the variables.

**Table 1: Summary of variables.**

Variables	Number of subjects (%)	
Age (in years)	≤ 10	1 (2.5%)
	11-20	2 (5%)
	21-30	8 (20%)
	31-40	9 (22.5%)
	41-50	5 (12.5%)
	51-60	8 (20%)
	61-70	3 (7.5%)
	≥ 71	4 (10%)
<b>Variables</b>	<b>Number of subjects (%)</b>	

<b>Sex</b>	Female	17 (42.5%)
	Male	23 (57.5%)
<b>Supra/Infartentorial</b>	Infarterntorial	3 (7.5%)
	Supratentorial	37 (92.5%)
<b>T1</b>	Heterogeneously Hypointense	31 (77.5%)
	Hypointense	3 (7.5%)
	Isointense	6 (15%)
<b>T2</b>	Heterogeneously Hyperintense	37 (92.5%)
	Hyperintense	3 (7.5%)
<b>Flair</b>	Heterogeneously hyperintense	37 (97.5%)
	Hyperintense	1 (2.5%)
<b>Diffusion Restriction</b>	Absent	28 (70%)
	Patchy diffusion	12 (30%)
<b>SWI</b>	Blooming	9 (22.5%)
	No blooming	31 (77.5%)
<b>Post-contrast study</b>	Heterogeneous enhancement	5 (12.5%)
	Minimal enhancement	8 (20%)
	No enhancement	10 (25%)
	Patchy enhancement	17 (42.5%)
<b>White matter tracts</b>	Destruction	12 (30%)
	Displacement	23 (57.5%)
	Infiltration	4 (10%)
	Normal	1 (2.5%)

In study 37 (92.5%) patients show the supratentorial location of the tumor and 3(7.5%) patients show the infratentorial location of the tumor. On T1 W 31 (77.5%) patients show heterogeneously hypointense signal, 6 (15%) patients show isointense signal and 3 (7.5%)

show hypointense signal. On T2 W 37 (92.5 %) patients show heterogeneously hyperintense signal and 3 (7.5%) patients show hyperintense signal. On FLAIR 37(97.5%) patients show heterogeneously hyperintense signal and 1(2.5%) patient showed a hyperintense signal as shown in table 1.

In study 28 (70%) patients show no diffusion restriction and 12 (30%) patients show patchy diffusion restriction. On SWI 9 (22.5%) patients are showing blooming and 31 (77.5%) patients show no blooming, blooming represents hemorrhage which is seen in high-grade gliomas. In the post-contrast enhancement study 17 (42.5%) patients show patchy enhancement, 8 (20%) patients showed minimal enhancement, 5 (12.5%) patients showed heterogenous enhancement, and 10(25%) shows no enhancement.

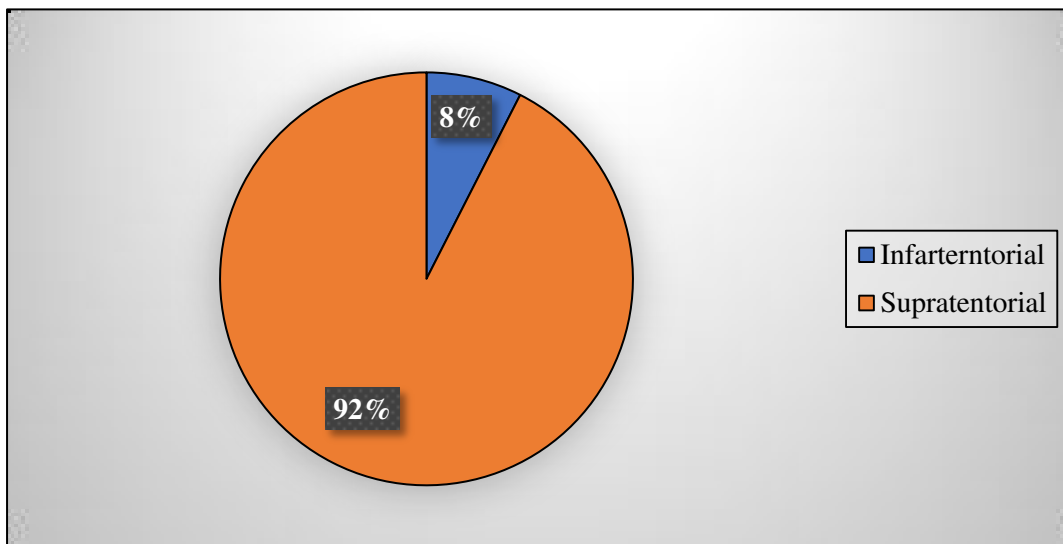


Chart 1: Pie chart showing the distribution of subjects by Supra/ Infratentorial

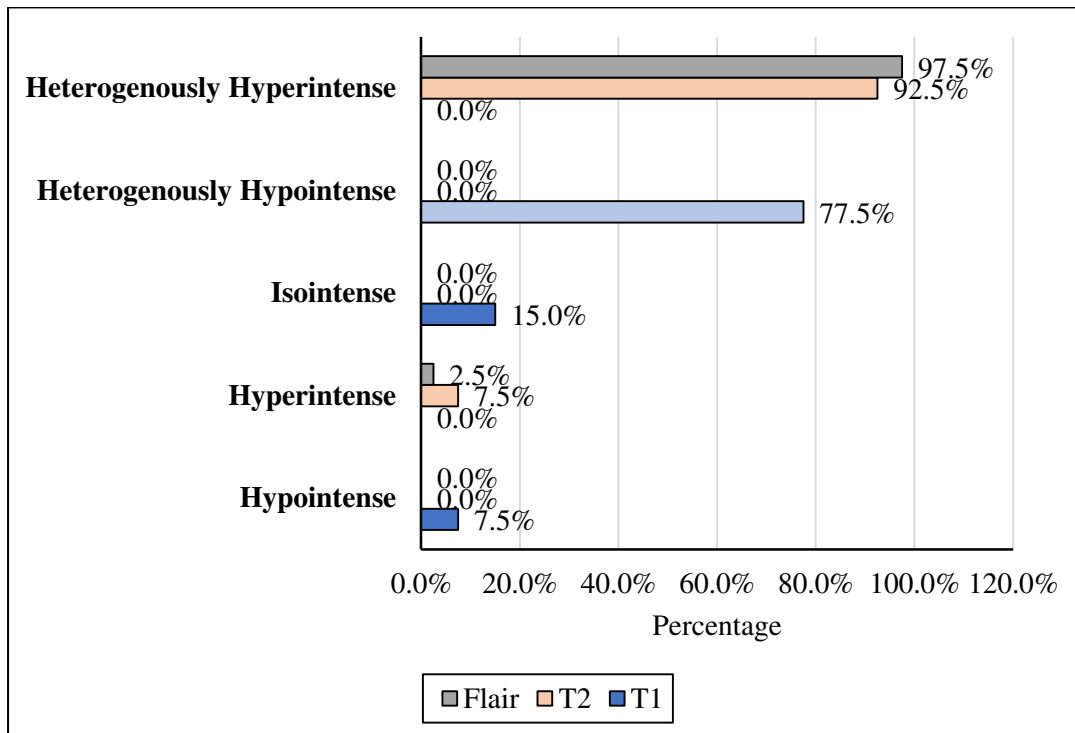


Chart 2: Bar graph showing the distribution of subjects by T1, T2, and Flair.

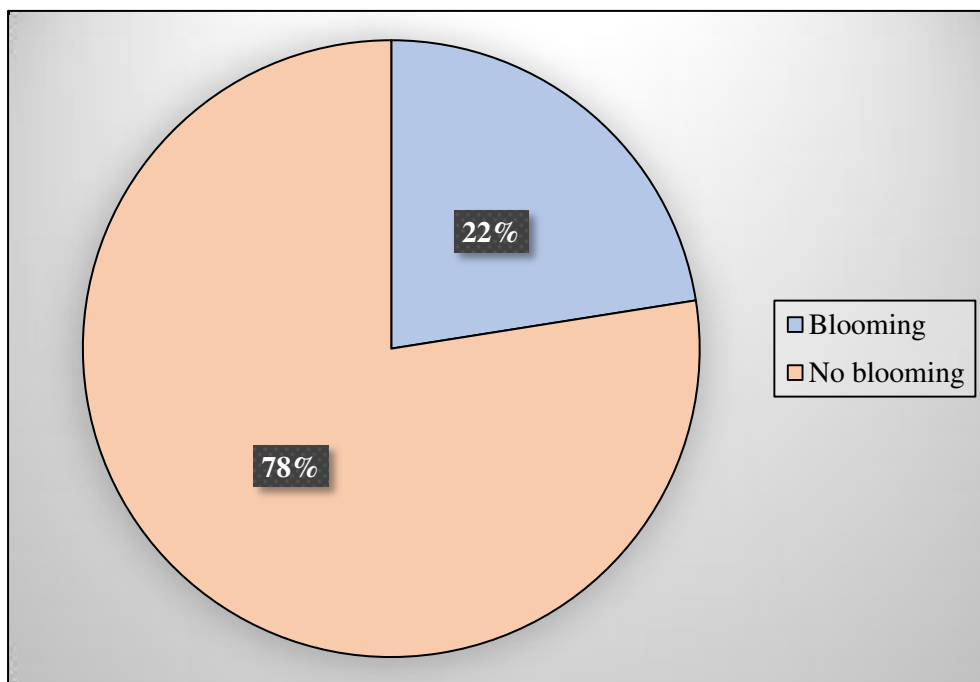


Chart 3: Pie chart showing the distribution of subjects by SWI

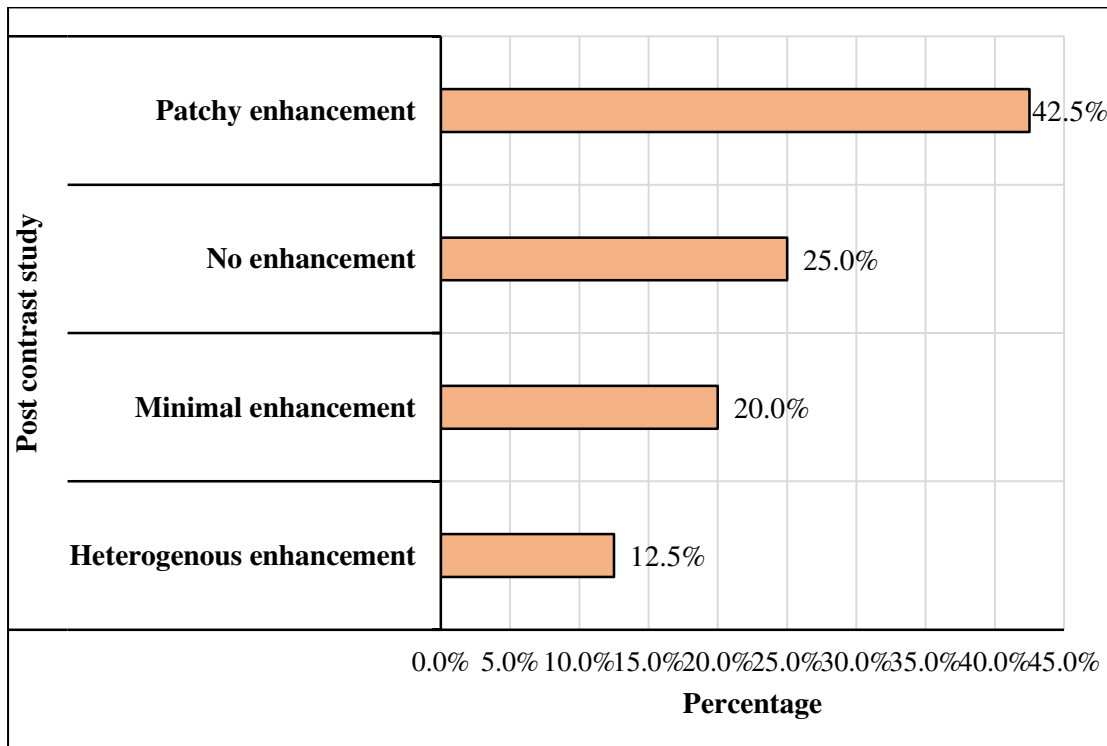


Chart 4: Bar graph showing the distribution of post-contrast study.

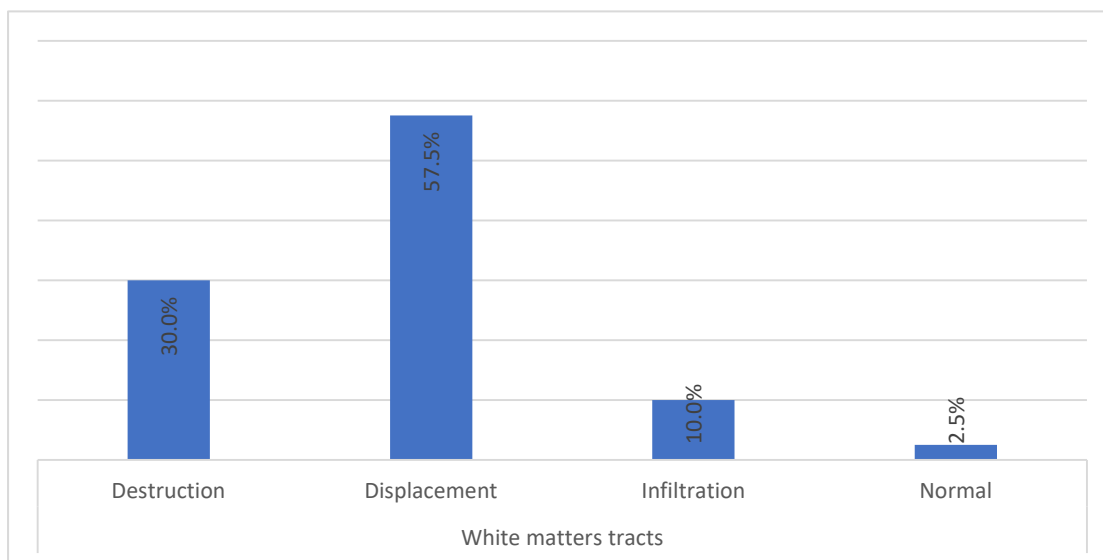


Chart 5: Bar graph showing the distribution of subjects by white matter tracts.

The below table compares some variables with the grades of the tumors.



**Table 2: Comparison of variables over the grade of the tumor.**

Variable	Grade of Tumor		p-value
	Low	High	
Age (in years)	38.83±15.81	49.81±19.8	0.05928 <sup>t</sup>
rCBV	0.83±0.57	3.87±1.61	<0.00001* <sup>MW</sup>
	1.3 (1.1, 5.1)	6.05 (1.2, 7.2)	
Cho/cr	1.85±0.58	5.13±1.9	<0.00001* <sup>MW</sup>
	1.61 (1.58, 4.2)	5.3 (1.6, 8.1)	
Cho/NAA	1.58±0.84	5.29±1.84	<0.00001* <sup>MW</sup>
	1.3 (1.1, 5.1)	6.05 (1.2, 7.2)	
Fractional anisotropy	0.12±0.02	0.16±0.03	<0.00001* <sup>t</sup>
	0.11 (0.1, 0.16)	0.17 (0.1, 0.19)	

Abbreviations: MW: Mann-Whitney test, t: t-test.

There is no significant difference in the mean of age over the grade of the tumor by a two-sample t-test.

By the Mann-Whitney test, there is a significant difference in the distribution of rCBV, Cho/cr, and Cho/NAA over the grade of the tumor.

By one-tailed t-test, the mean of fractional anisotropy is significantly more in high-grade tumors compared to low-grade tumors.

The below plots visualize the same.

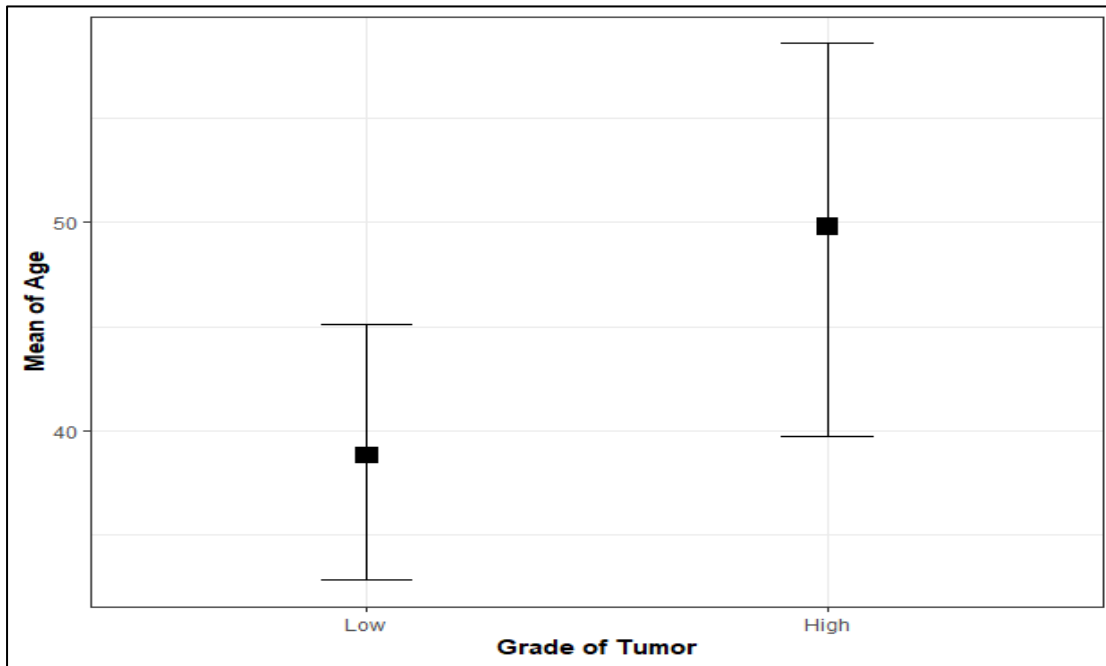


Chart 6: Box whisker plot showing mean of age over the grade of the tumor.

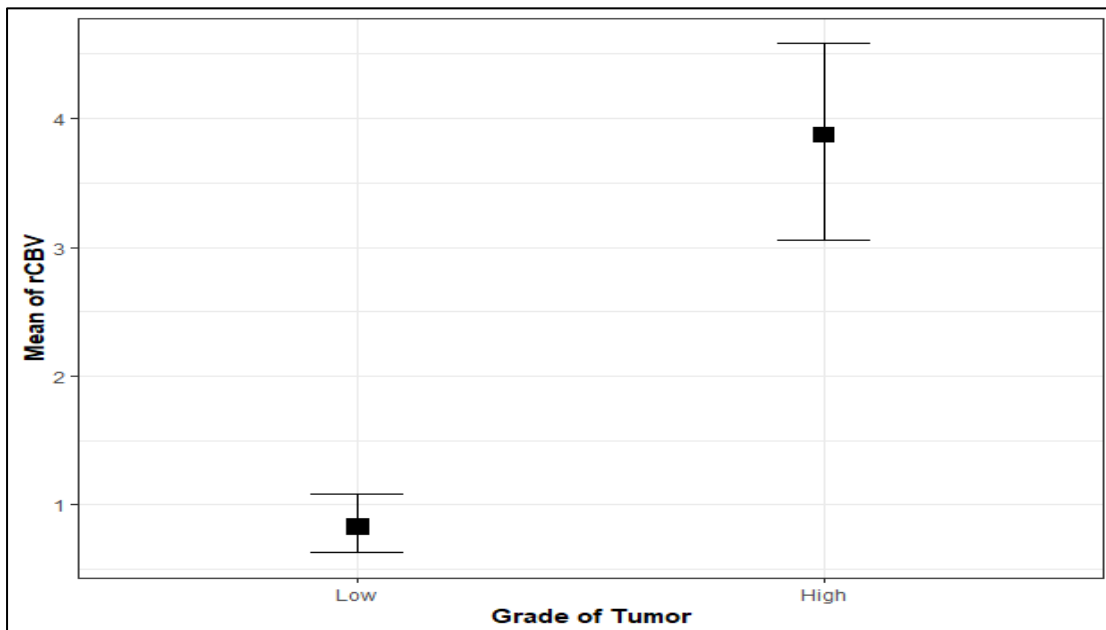


Chart 7: Box whisker plot showing mean of rCBV over the grade of the tumor.

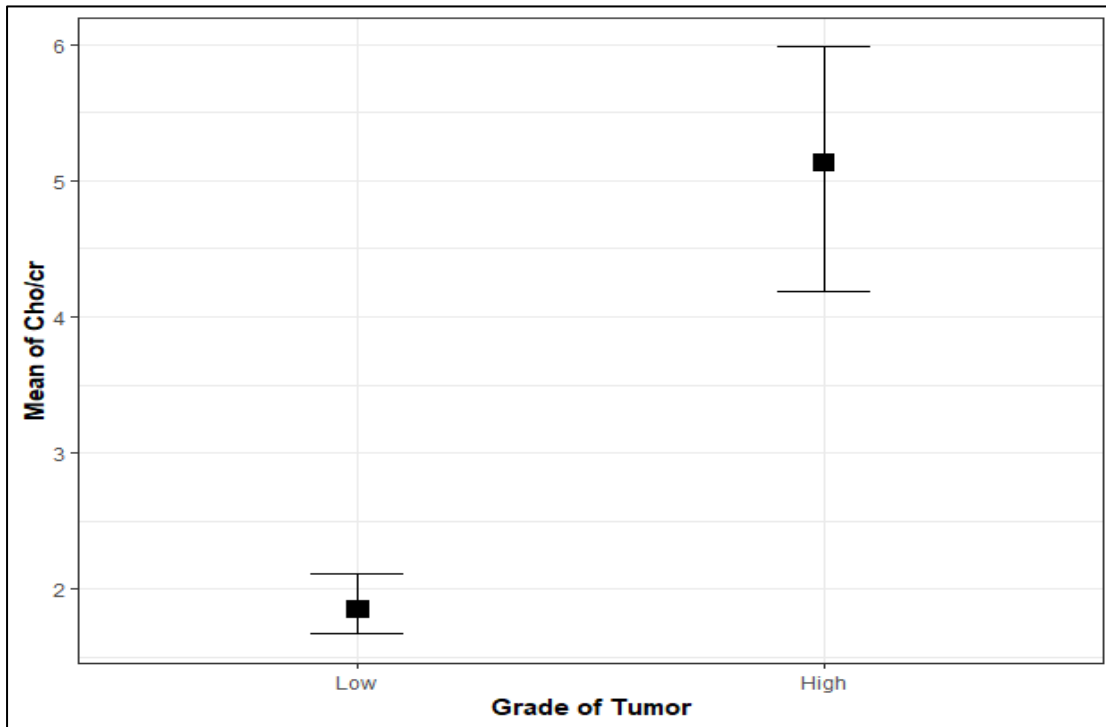


Chart 8: Box whisker plot showing the mean of Cho/Cr over the grade of the tumor.

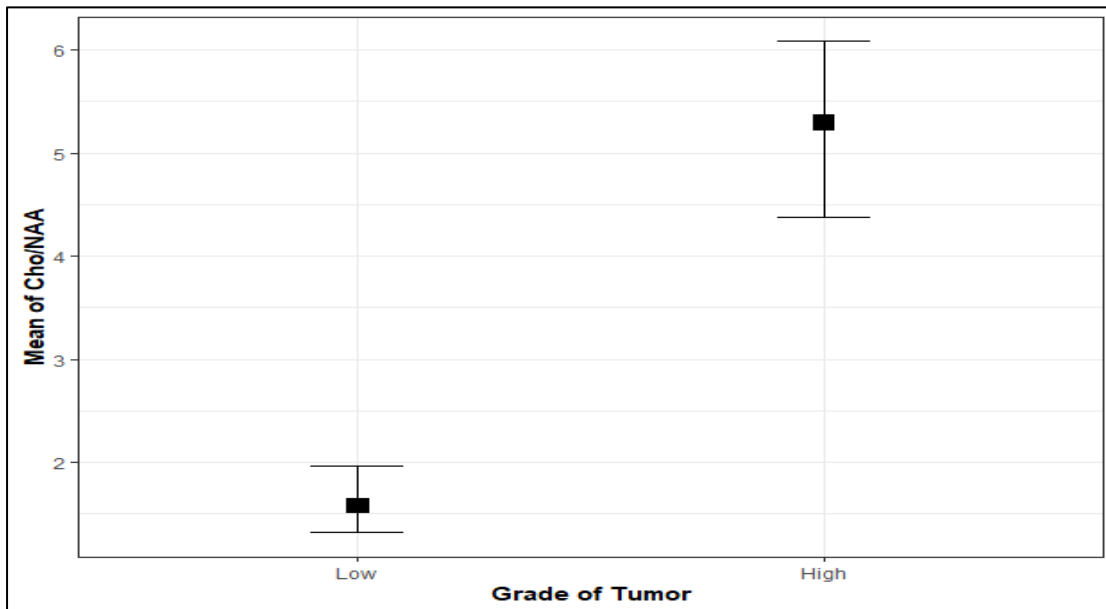


Chart 9: Box whisker plot showing the mean of Cho/NAA over the grade of the tumor.

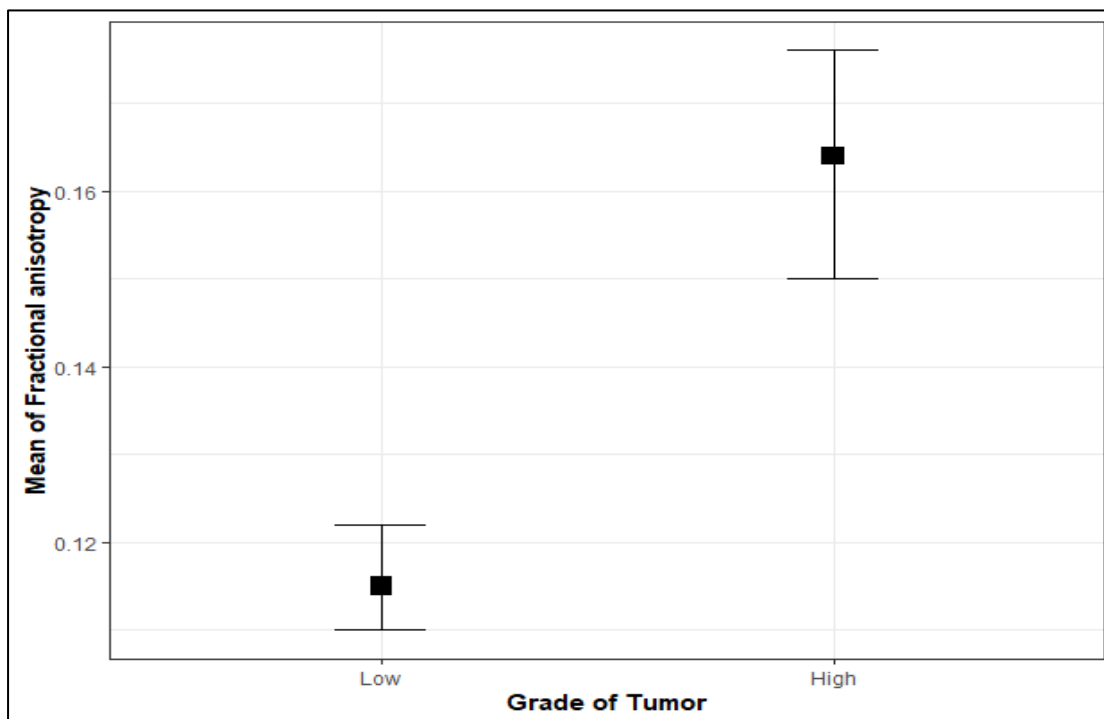


Chart 10: Box whisker plot showing mean of Fractional anisotropy over the grade of the tumor.

Table 3: Cut-off value and other diagnostic values in predicting low/high-grade tumors.

Variable	Cut-off	Sensitivity	Specificity	PPV	NPV	AUC (CI)
rCBV	>1.7	91.6%	87.5%	91.7%	87.5%	0.879 (0.722, 1)
Cho/Cr	>1.81	87.5%	87.5%	91.3%	82.3%	0.895 (0.762, 1)
Cho/NAA	>2.8	95.8%	87.5%	92%	93.3%	0.892 (0.752, 1)
Fractional anisotropy	> 0.14	91.7%	87.5%	91.7%	87.5%	0.887 (0.744, 1)

Abbreviations: PPV: Positive predictive value, NPV: Negative predictive value, AUC: Area under a curve, CI: Confidence interval

**DISCUSSION**

In the study, there is no significant difference in the mean of age over the grade of the tumor by applying a two-sample t-test in which the mean age for high-grade gliomas is (49.8±19.8) and low-grade gliomas are (38.83± 15.81) and found no significant difference (P = 0.05928) in the distribution of grades of tumor in our study.

By the Mann-Whitney test, there is a significant difference in the distribution of rCBV, Cho/cr, and Cho/NAA over the grade of the tumor.

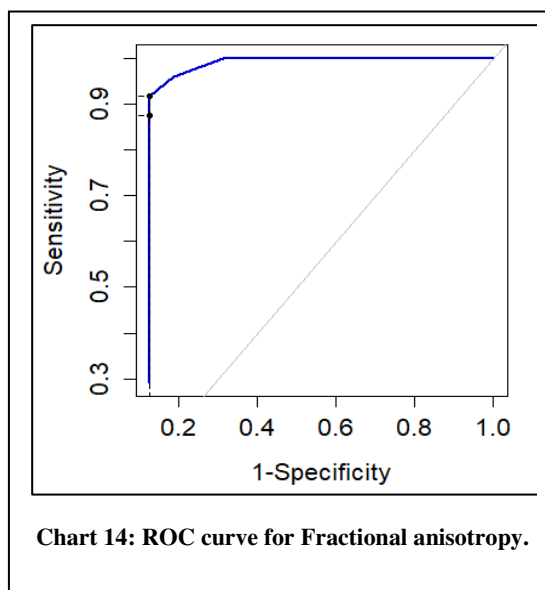
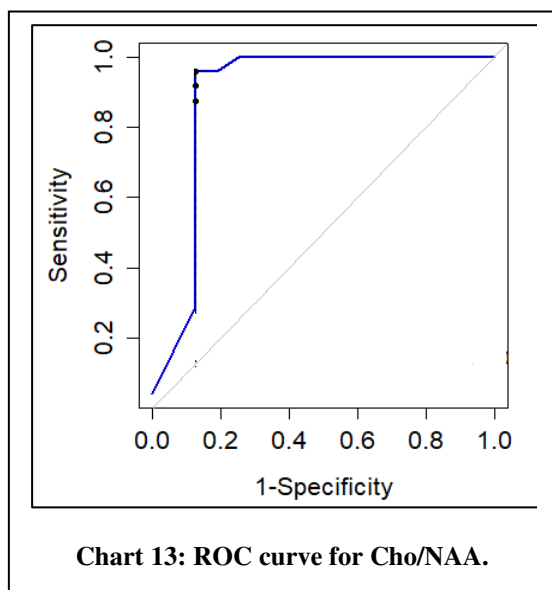
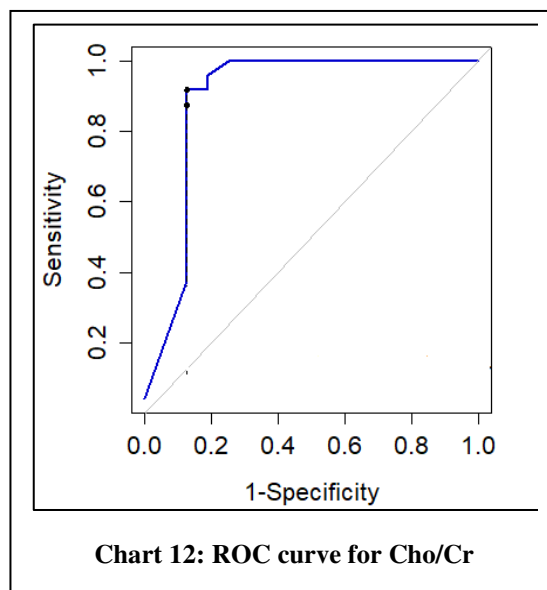
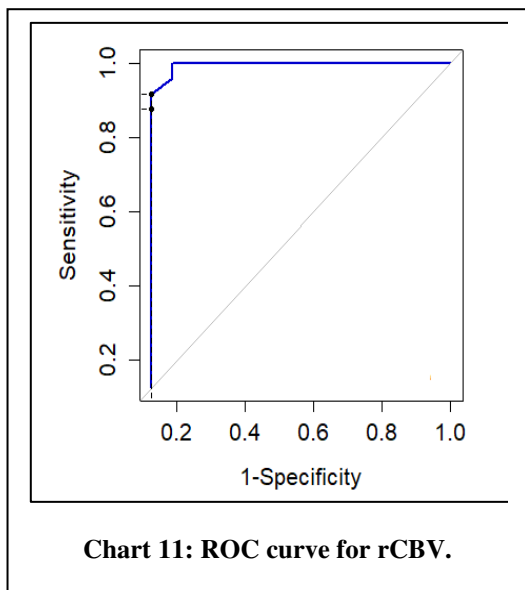
At an intermediate TE on spectroscopy, there is a significant statistical difference ( $P < 0.00001$ ) in the values obtained for Cho/cr and Cho/NAA metabolites for different grades of tumors. In agreement with our results, faten et al, Fatima et al and Naser et al reported that Cho/NAA and Cho/Cr ratios show a statistically significant increase in high-grade tumors compared to low-grade tumors<sup>12-18</sup>.

The present study disclosed that for high-grade gliomas Cho/Cr ratios with mean average values of  $5.13 \pm 1.9$  ranging from 1.6 to 8.1 and median value of 5.3 and Cho/NAA ratios with mean average values of  $5.29 \pm 1.84$  ranging from 1.2 to 7.2 and the median value is 6.05. Similarly, Cho/Cr ratios for low-grade tumors range with mean average values  $1.85 \pm 0.58$  ranging from 1.58 to 4.2 and a median value of 1.61, and Cho/NAA ratios with mean average values of  $1.58 \pm 0.84$  ranging from 1.1 to 5.1 and median value are 1.3.

In the perfusion study rCBVt values for tumors, there is a significant statistical difference ( $P < 0.00001$ ) for high-grade and low-grade gliomas, the high-grade gliomas show mean average rCBVt values of  $3.87 \pm 1.61$  ranging from 1.2 to 7.2 and median value of 6.05 and low-grade gliomas shows mean average rCBVt values  $0.83 \pm 0.57$  ranging from 1.1 to 5.1 and median value of 1.3. The results agreed with other studies by Fatima et al<sup>12</sup>, Eman et al<sup>19</sup> and Soliman et al<sup>20</sup>.

By one-tailed t-test, the mean of fractional anisotropy is significantly more in high-grade

tumors compared to low-grade tumors. In diffuse tensor imaging {DTI }



study fractional anisotropy values show a significant statistical difference ( $p < 0.00001$ ) between high-grade and low-grade gliomas. The fractional anisotropy values for high-grade gliomas show mean values of  $0.16 \pm 0.03$  ranging from 0.1 to 0.19 with a median value of 0.17, low-grade gliomas show mean values of  $0.12 \pm 0.02$  ranging from 0.1 to 0.16 with the median value of 0.11. The results agreed with other studies by Lobel et al<sup>21</sup> and Kang et al<sup>22</sup>.

In the study using ROC analysis the cut-off values for intermediate TE Cho metabolites ratios were used to differentiate high-grade tumors from low-grade tumors; cut-off values for Cho/Cr ratio  $> 1.1$  and Cho/NAA  $> 2.8$  with higher values considered as high-grade gliomas<sup>14-18</sup>. The sensitivity and specificity for Cho/Cr are 87.5 % & 87.5% respectively and for Cho/NAA 95.8% & 87.5% respectively. At an intermediate TE, our results revealed that the

sensitivity of Cho/NAA was 95.8 %, indicating true positive high rates and false negative low rates; therefore, it is very useful for determining high-grade tumors. The corresponding specificity of this ratio was 87.5%, indicating that the less severe tumors were correctly classified. The sensitivity and specificity of Cho/Cr are less compared to Cho/NAA and was 87.5 %, indicating less true positive high rates and more false negative low rates compared to Cho/NAA; The corresponding specificity of this ratio was 87.5%, indicating that the less severe tumors were correctly classified. Positive predictive value (PPV), Negative predictive value (NPV), and Area under the curve (AUC){CI} for Cho/Cr are 91.3%, 82.3% & 0.895 {0.762,1} respectively and for Cho/NAA are 92%, 93.3% & 0.892 {0.752,1} respectively.

In the study using ROC analysis, the cut-off values for rCBVt were used to differentiate high-grade and low-grade tumors; cut-off values for rCBVt > 1.7 with higher values considered as high-grade gliomas<sup>1,3,28,20</sup>. Another important finding is that the rCBVt value with a threshold of more than 1.7 can differentiate between LGG and HGG and gives 91.6% sensitivity, 87.5% specificity, and 96% diagnostic accuracy. The 91.6 specificity reflects a high real negative rate which means that most LGGs have been correctly diagnosed. The relatively high sensitivity means that even though few have been misclassified, most HGGs have been correctly diagnosed. These results reflect those of Fatima et al. who also found that LG and HG could be differentiated from rCBV at the cut-off of 1.33 were 100%, 67%, and 90% respectively<sup>23</sup>. Positive predictive value (PPV), Negative predictive value (NPV), and Area under the curve (AUC){CI} for rCBVt are 91.7%, 87.5% & 0.879 {0.722,1} respectively.

In the study using ROC analysis, the cut-off values for DTI (FA) were used to differentiate high-grade and low-grade tumors; cut-off values for FA > 0.14 with higher values were considered high-grade gliomas. The sensitivity and specificity for FA are 91.7 % & 87.5 % respectively. The FA values in these regions of both HGG and LGG were lower than those of contralateral NAWM or corpus callosum which was consistent with prior studies<sup>24,25,26</sup>. The FA value is an indicator of white matter integrity and decreased FA was putative destruction of the white matter tract. Inoue T et al<sup>27</sup> found that the FA values in the solid portion of HGG were significantly higher than those of LGG. High anisotropy implies that the tissue is symmetric and histologically organized. It may influence the anisotropy and increase the FA value the 87.5 specificity reflects a high real negative rate which means that most LGGs have been correctly diagnosed. Positive predictive value (PPV), Negative predictive value (NPV), and Area under the curve (AUC){CI} for FA are 91.7%, 87.5% & 0.887 {0.744,1} respectively

The current study had some limitations

- 1-Relatively small sample size (40 cases)
- 2-pediatric cases were significantly fewer in the study group.
- 3-This study is missing some categories like less number of infratentorial lesions and extra-axial brain tumors.

#### Recommendations

Further large-scale research is needed to assess the use of advanced MRI imaging

sequences to aid in the differentiation between low-grade and high-grade Gliomas.

## SUMMARY

We have studied the role of advanced MRI imaging in differentiating high-grade and low-grade gliomas. Our study shows significant statistical differences in a p-value for various advanced MRI imaging sequences like perfusion study, spectroscopy study, and diffuse tensor imaging in predicting high-grade versus low-grade tumors in comparison with previous studies. The sensitivity and specificity for Cho/Cr are 87.5 % & 87.5% and for Cho/NAA are 95.8% & 87.5% respectively. An important finding is that the rCBVt value with a threshold of more than 1.7 can differentiate between LGG and HGG and gives 91.6% sensitivity, and 87.5% specificity respectively. The sensitivity and specificity for FA are 91.7 % & 87.5 % respectively. The positive predictive value (PPV) and negative predictive values (NPV) for rCBVt, Cho/Cr, Cho/NAA, and fractional anisotropy are 91.7% & 87.5%, 91.3% & 82.3%, 92% & 93.3% and 91.7% & 87.5% respectively. The cut-off values for rCBV t, Cho/Cr, Cho /NAA, and FA are >1.7, >1.81, >2.8, and >0.14 respectively with a higher value for high-grade gliomas. There is a significant statistical difference in the distribution of rCBVt, Cho/Cr, and Cho/NAA by the Mann-Whitney test over the grading of tumors. By one-tailed t-test, the mean of fractional anisotropy is significantly more in high-grade tumors compared to low-grade tumors.

## Conclusion

We concluded that the utility of advanced MRI imaging can effectively differentiate different grades of brain tumors. The advanced MRI imaging methods-perfusion study, spectroscopy, and diffuse tensor imaging have a significant correlation with the degree of malignancy, thus predicting different grades of tumors compared to conventional MRI imaging alone, aiding in management and follow-up. In addition to conventional imaging, the use of advanced MRI imaging sequences in brain tumor imaging provides significant insight into tumor malignancy. These are non-invasive, easily accessible techniques that aid in patient prognosis and thus avoid unnecessary stereotactic biopsies for low-grade gliomas that require follow-up. The use of advanced MRI imaging sequences in brain tumors to differentiate between tumor grades is an important part of patient management.

## References

1. Caulo M, Panara V, Tortora D, Mattei PA, Briganti C, Pravata E et al (2014) Data-driven grading of brain gliomas: a multiparametric MR imaging study. *Radiology*. 272(2):494–503
2. Di Costanzo A, Pollice S, Trojsi F, Giannatempo GM, Popolizio T, Canalis L et al (2008) Role of perfusion-weighted imaging at 3 Tesla in the assessment of malignancy of cerebral gliomas. *Radiol Med*. 113(1):134–143
3. Morita N, Wang S, Chawla S, Poptani H, Melhem ER (2010) Dynamic susceptibility contrast perfusion weighted imaging in grading of nonenhancing astrocytomas. *J Magn Reson Imaging*. 32(4):803–808
4. Vamvakas A, et al. imaging biomarker analysis of advanced multiparametric MRI for glioma grading. *Physica Medica*. 2019; 60:188–98.
5. Sjobakk TE, Lundgren S, Kristoffersen A, Singstad T, Svarliaunet AJ, Sonnewald U et al (2006) Clinical 1H magnetic resonance spectroscopy of brain metastases at 1.5T



- and 3T. *Acta Radiol.* 47(5):501–508.
6. Poot DH, den Dekker AJ, Achten E, Verhoye M, Sijbers J. Optimal experimental design for diffusion kurtosis imaging. *IEEE Trans Med Imaging* 2010; 29(3):819–829.
  7. Wu EX, Cheung MM. MR diffusion kurtosis imaging for neural tissue characterization. *NMR Biomed* 2010; 23(7):836–848.
  8. Hui ES, Cheung MM, Qi L, Wu EX. Towards better MR characterization of neural tissues using directional diffusion kurtosis analysis. *Neuroimage* 2008; 42(1):122–134.
  9. Jensen JH, Helpern JA, Ramani A, Lu H, Kaczynski K. Diffusional kurtosis imaging: the quantification of non-Gaussian water diffusion by means of magnetic resonance imaging. *MagnReson Med* 2005; 53(6):1432–1440.
  10. Fieremans E, Jensen JH, Helpern JA. White matter characterization with diffusional kurtosis imaging. *Neuroimage* 2011; 58(1):177–188.
  11. Dumas-Duport C, Scheithauer B, O’Fallon J, Kelly P. Grading of astrocytomas: a simple and reproducible method. *Cancer* 1988; 62(10):2152–2165.
  12. de Fatima Vasco Aragao M, Law M, Batista de Almeida D, Fatterpekar G, Delman B, Bader AS et al (2014) Comparison of perfusion, diffusion, and MR spectroscopy between low-grade enhancing pilocytic astrocytomas and high-grade astrocytomas. *AJNR Am J Neuroradiol.* 35(8):1495 –1502
  13. Naser RKA, Hassan AAK, Shabana AM, Omar NN (2016) Role of magnetic resonance spectroscopy in grading of primary brain tumors. *Egypt J RadiolNucl Med.* 47(2):577 –584 24.
  14. Kousi E, Tsougos I, Tsolaki E, Fountas KN, Theodorou K, Fezoulidis I et al (2012) Spectroscopic evaluation of glioma grading at 3T: the combined role of short and long TE. *ScientificWorldJournal.* 2012:546171
  15. Liu ZL, Zhou Q, Zeng QS, Li CF, Zhang K (2012) Noninvasive evaluation of cerebral glioma grade by using diffusion-weighted imaging-guided singlevoxel proton magnetic resonance spectroscopy. *J Int Med Res.* 40(1):76–84
  16. Toyooka M, Kimura H, Uematsu H, Kawamura Y, Takeuchi H, Itoh H (2008) Tissue characterization of glioma by proton magnetic resonance spectroscopy and perfusion-weighted magnetic resonance imaging: glioma grading and histological correlation. *Clin Imaging.* 32(4):251 –258
  17. Zeng Q, Liu H, Zhang K, Li C, Zhou G (2011) Noninvasive evaluation of cerebral glioma grade by using multivoxel 3D proton MR spectroscopy. *MagnReson Imaging.* 29(1):25 –31
  18. Zonari P, Baraldi P, Crisi G (2007) Multimodal MRI in the characterization of Glial neoplasms: the combined role of single-voxel MR spectroscopy, diffusion imaging and echo-planar perfusion imaging. *Neuroradiology.* 49(10):795 –803
  19. Geneidi EASH, Habib LA, Chalabi NA, Haschim MH (2016) Potential role of

- quantitative MRI assessment in differentiating high from low-grade gliomas. *Egypt J RadiolNucl Med.* 47(1):243 –253.
20. Soliman RK, Gamal SA, Essa AA, Othman MH (2018) Preoperative grading of glioma using dynamic susceptibility contrast MRI: relative cerebral blood volume analysis of intra-tumoural and peritumoural tissue. *Clin Neurol Neurosurg.* 167:86 – 92.
  21. Löbel U, Sedlacik J, Güllmar D, Kaiser WA, Reichenbach JR, Mentzel HJ. Diffusion tensor imaging: the normal evolution of ADC, RA, FA, and eigenvalues studied in multiple anatomical regions of the brain. *Neuroradiology* 2009;51(4):253–263.
  22. Kang X, Herron TJ, Woods DL. Regional variation, hemispheric asymmetries and gender differences in pericortical white matter. *Neuroimage* 2011;56(4):2011–2023.
  23. Server A, Orheim TE, Graff BA, Josefsen R, Kumar T, Nakstad PH (2011) Diagnostic examination performance by using microvascular leakage, cerebral blood volume, and blood flow derived from 3-T dynamic susceptibility-weighted contrast-enhanced perfusion MR imaging in the differentiation of glioblastoma multiforme and brain metastasis. *Neuroradiology.* 53(5):319 –330.
  24. Tropine A, Vucurevic G, Delani P, et al. Contribution of diffusion tensor imaging to delineation of gliomas and glioblastomas. *J MagnReson Imaging* 2004; 20(6):905–912 37.
  25. Lee HY, Na DG, Song IC, Lee DH, Seo HS, Kim JH, et al. Diffusion-tensor imaging for glioma grading at 3-T magnetic resonance imaging: analysis of fractional anisotropy and mean diffusivity. *J Comput Assist Tomogr* 2008; 32: 298-303.
  26. Beppu T, Inoue T, Shibata Y, et al. Measurement of fractional anisotropy using diffusion tensor MRI in supratentorial astrocytic tumors. *J Neurooncol* 2003;63(2):109–116.
  27. Inoue T, Ogasawara K, Beppu T, Ogawa A, Kabasawa H. Diffusion tensor imaging for preoperative evaluation of tumor grade in gliomas. *Clin Neurol Neurosurg* 2005; 107: 174-80.
  28. Kikuchi K, Hiwatashi A, Togao O, Yamashita K, Kamei R, Kitajima M et al (2018) Usefulness of perfusion- and diffusion-weighted imaging to differentiate between pilocytic astrocytomas and high-grade gliomas: a multicenter study in Japan. *Neuroradiology.* 60(4):391 –401